adhesive joints mixed mode testing analysis

F.J.P. Chaves

L.F.M. da Silva

M.F.S.F. de Moura

D. Dillard

CLBA 2012

CONFERÊNCIA LUSO-BRASILEIRA DE ADESÃO E ADESIVOS

outline

- Predict the structure toughness
- Joint mechanical behavior
- Adhesive fracture energies in Mode I, Mode II (and Mode III)

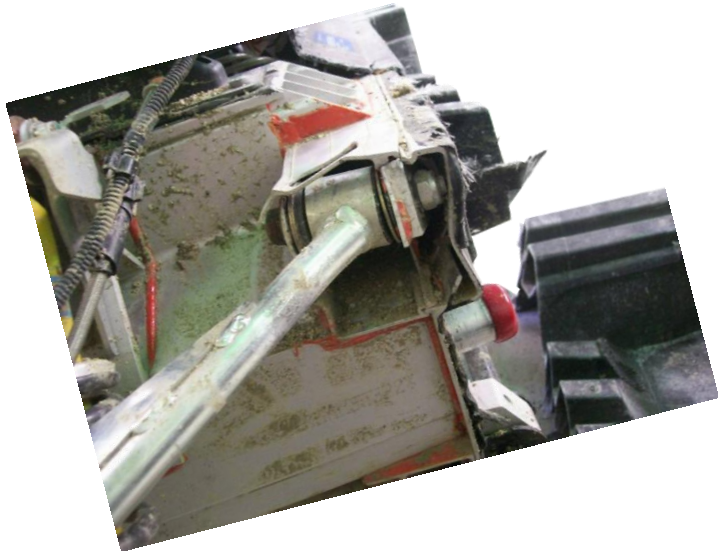

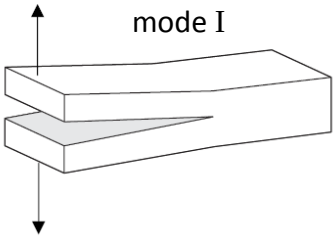

Mode I – opening mode (a tensile stress normal to the plane of the crack);

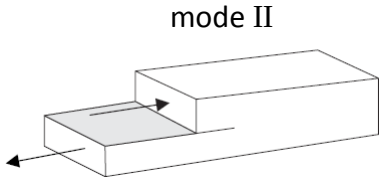

Mode II – sliding mode (a shear stress acting parallel to the plane of the crack and perpendicular to the crack front);

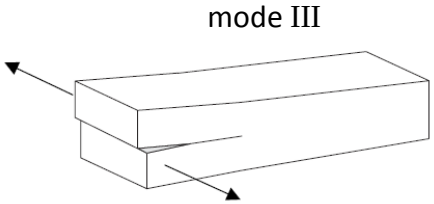

Mode III – tearing mode (a shear stress acting parallel to the plane of the crack and parallel to the crack front)

Mode I release rate energy G_I is well known and well characterized.

DCB – Double Cantilever Beam

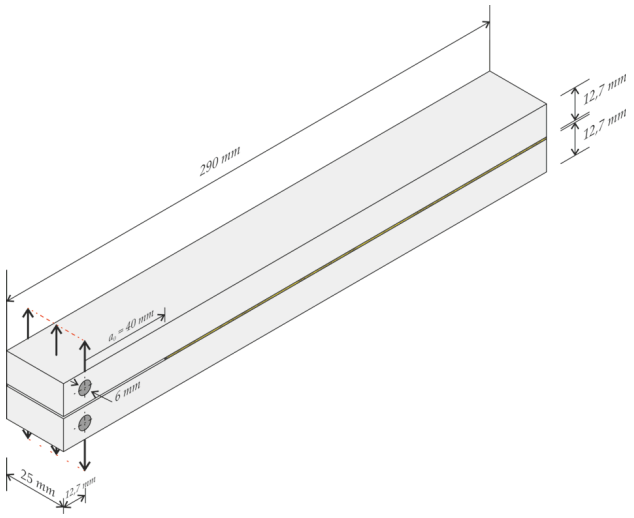

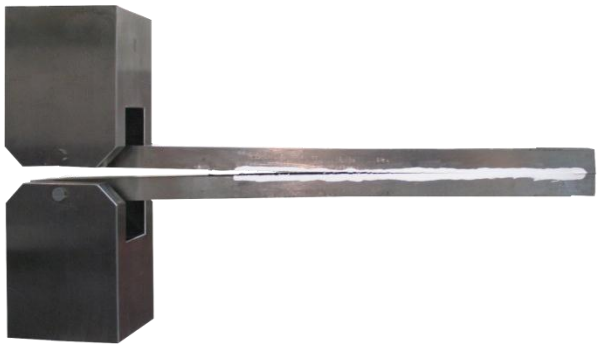

ASTM D 3433 - 99

TDCB – Tapered Double Cantilever Beam

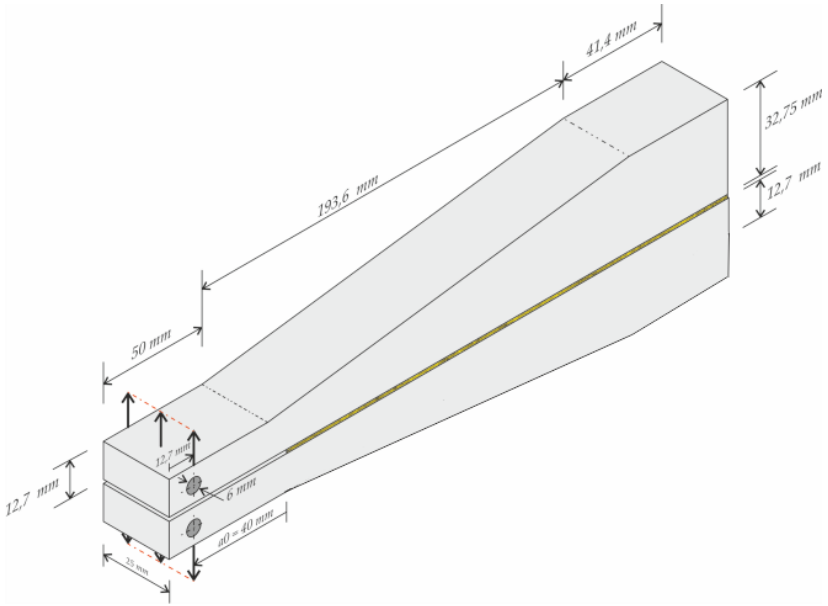

Mode II release rate energy G_{IIC} .

ENF – End Notch Flexure

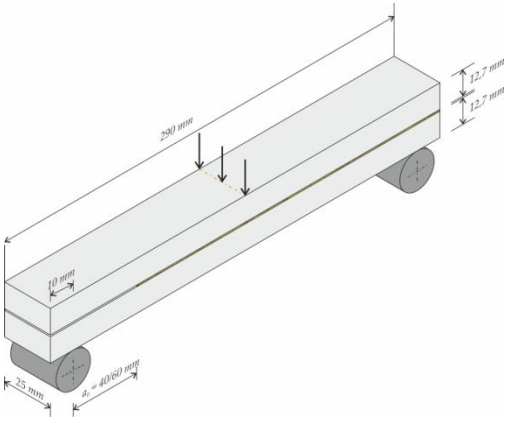

4ENF - 4 Points End Notch

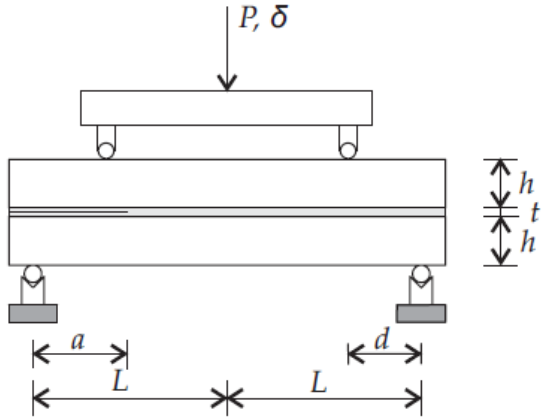

ELS – End Load Split

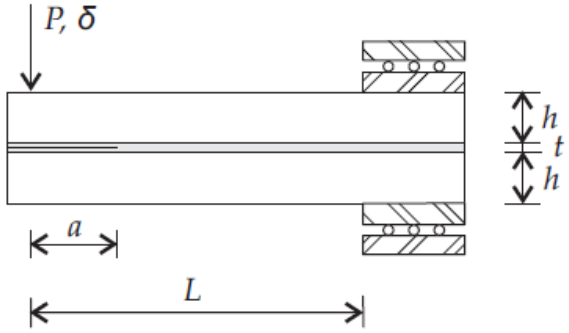

CLS - Crack Lap Shear

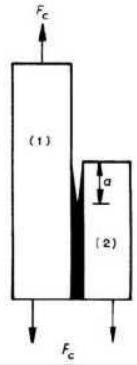

EDT - Edge Delamination Tension

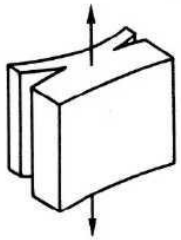

Arcan

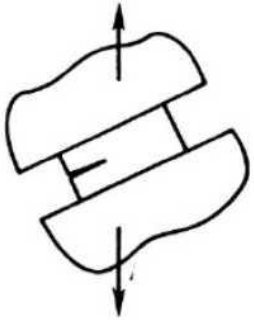

MMF - Mixed Mode Flexure

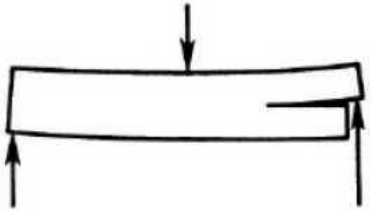

Mixed Mode Bending [MMB] **ASTM D6671**

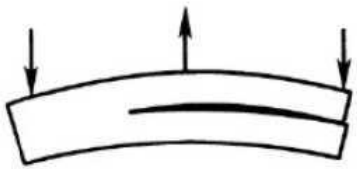

Asymmetrical Double Cantilever Beam [ADCB]

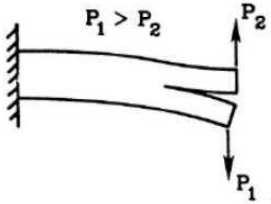

Asymmetrical Tapered Double Cantilever Beam [ATDCB]

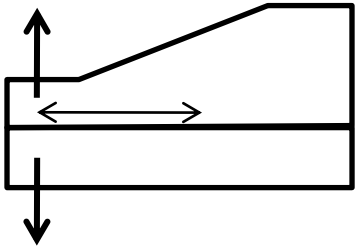

SLB – Single Leg Bending

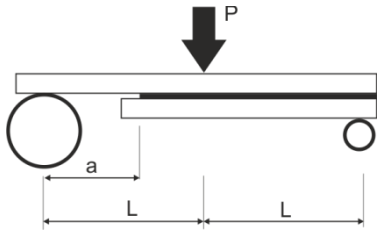

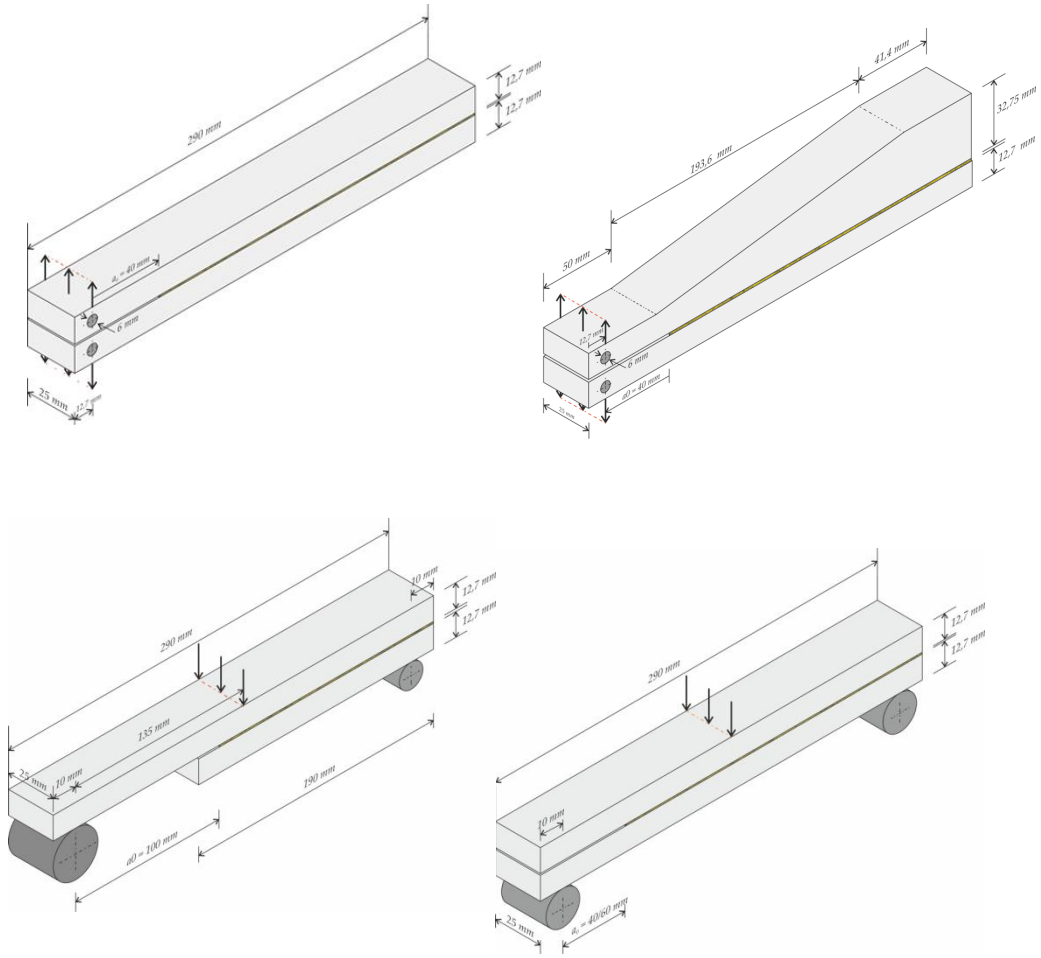

DCB, ATDCB, SLB and ENF specimen geometries.

Bondline thickness = 0.2 mm

Adhesive shear properties using the thick adherend shear test method ISO 11003-2

	2015
Shear modulus G (MPa)	487 ± 77
Shear yield strength τ_{ya} (MPa)	17.9 ± 1.80
Shear strength τ_r (MPa)	17.9 ± 1.80
Shear failure strain γ_f (%)	43.9 ± 3.40

Steel adherend properties

Steel	DIN 40CrMnNiMo7.
Young modulus, E [Gpa]	205
Yield strength, σ_y [MPa]	~ 900
Shear strength, σ_y [MPa]	~ 1000
Strain, ε_f [%]	~ 15

Fracture toughness obtained with the conventional testing methods (average and standard deviation).

Test type	G_{Ic} (N/mm)	G_{IIc} (N/mm)
DCB+	0.44 ± 0.05	–
ENF	–	2.1 ± 0.21
SLB*	0.34 ± 0.06	0.32 ± 0.06
ADCB*	0.41 ± 0.04	0.004 ± 0.0005
ATDCB*	0.32 ± 0.04	0.07 ± 0.006

\+ Value corresponding to CBBM

* For these tests, the values indicated correspond to G_I and G_{II} and not G_{Ic} and G_{IIc}.

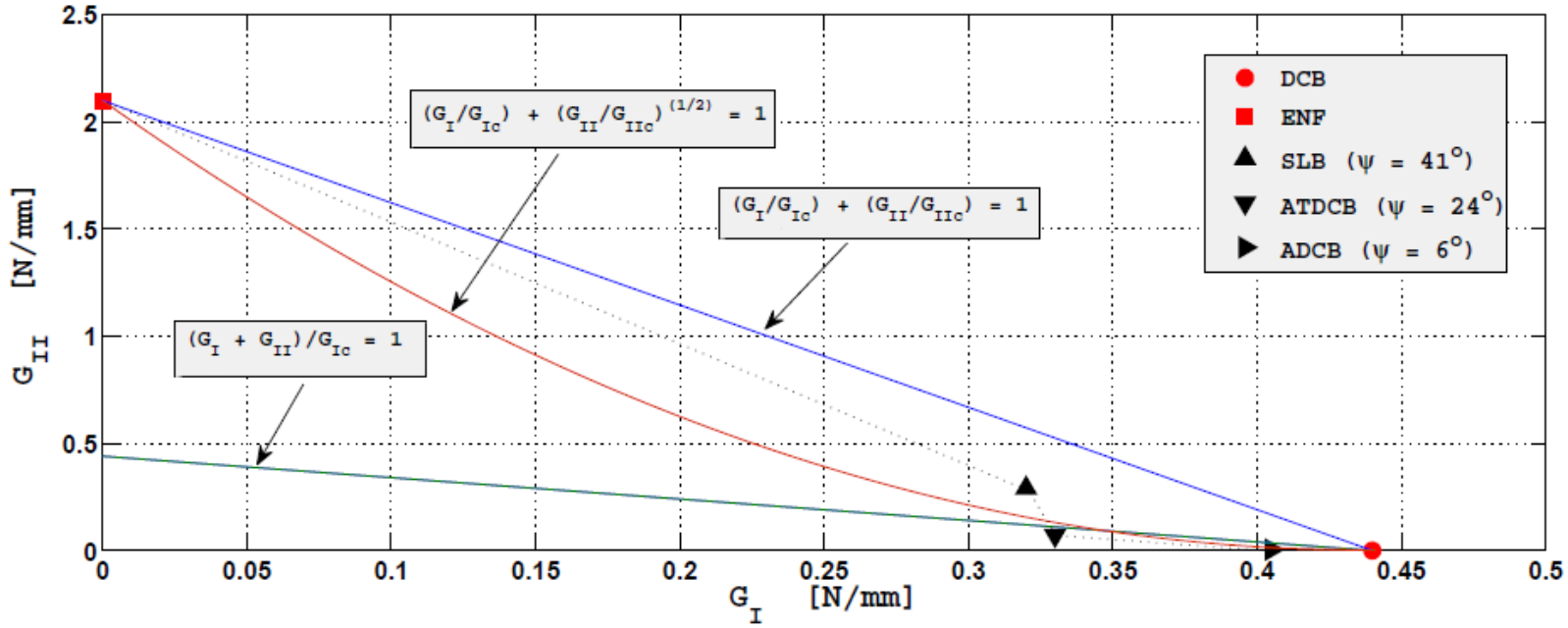

Fracture envelope for conventional tests.

Fracture toughness of a structural adhesive under mixed mode loadings

L.F.M. da Silva et al. / Mat.-wiss. u.Werkstofftech. 2011, 42, No. 5

Designation: D 6671/D 6671M

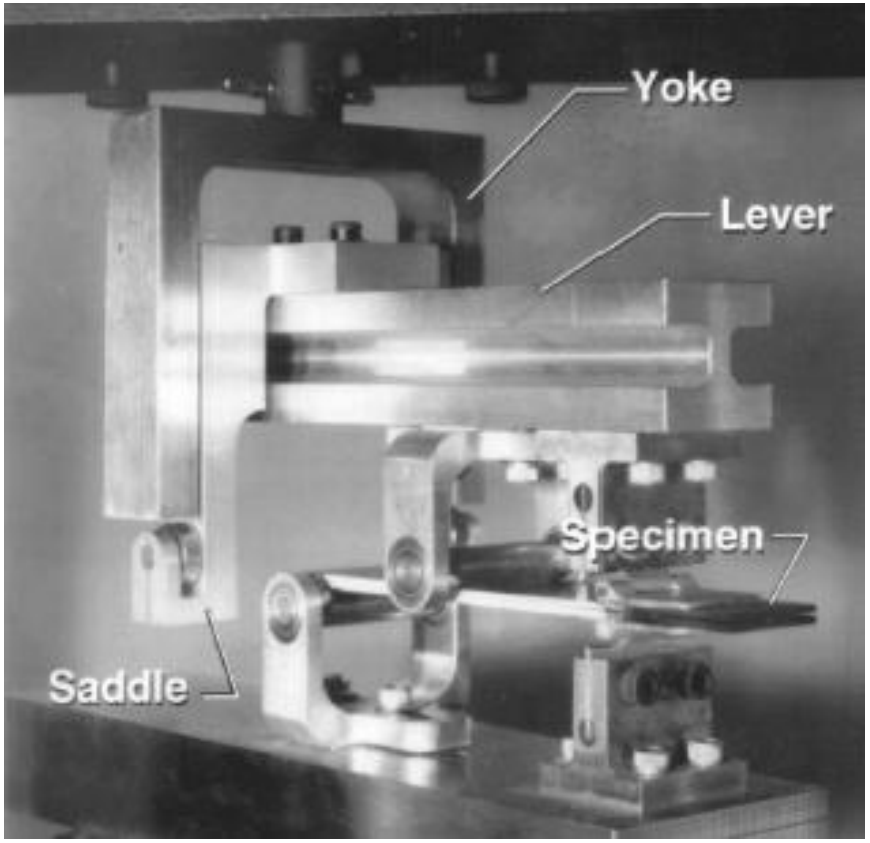

Modified Mixed Mode Bending by Reeder.

Compliance Based Beam Method applied to MMB

J.M.Q. Oliveira et al. / Composites Science and Technology **67** (2007) 1764–1771

$$G_I = \frac{12a_{eq,I}^2 P_I^2}{B^2 h^3 E_{fI}} + \frac{6P_I^2}{5B^2 hG} \quad (1)$$

$$G_{II} = \frac{9a_{eq,II}^2 P_{II}^2}{16B^2 h^3 E_{fII}} \quad (2)$$

An equivalent crack length ($a_{eq,I}$ and $a_{eq,II}$) can be obtained from the previous equation as a function of the measured current compliance $a_{eq,I} = f(C_I)$ and $a_{eq,II} = f(C_{II})$

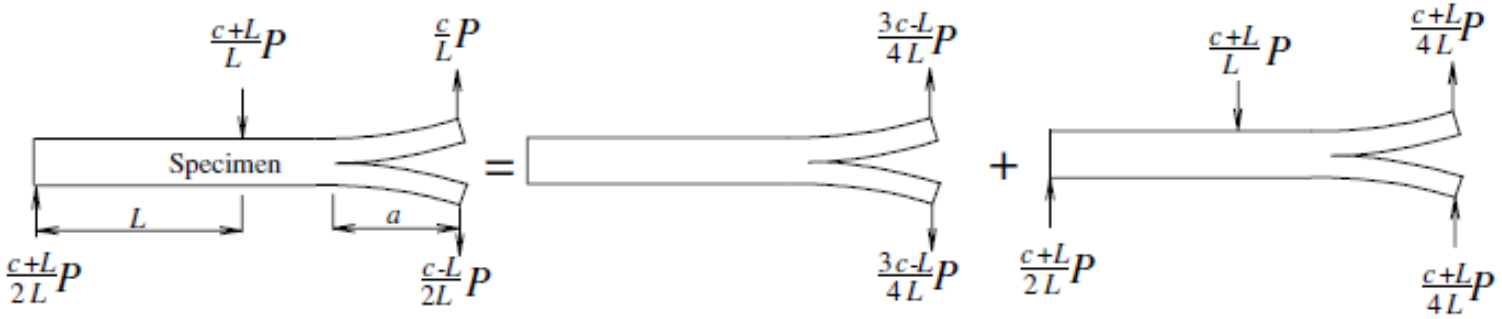

Schematic representation of loading in the MMB test.

J.M.Q. Oliveira et al. / Composites Science and Technology **67** (2007) 1764–1771

pure mode loading

$$P_{I} = \left(\frac{3c - L}{4L}\right)P \qquad P_{II} = \left(\frac{c + L}{L}\right)P \qquad (7)$$

The specimen was modelled with 11598 plane strain 8-node quadrilateral elements and 257 6-node interface elements with null thickness placed at the mid-plane of the bonded specimen.

ABAQUS®

Elastic and cohesive properties.

Elastic properties (Steel)		Cohesive properties (Adhesive)			
E (GPa)	G (MPa)	$s_{u,I}$ (MPa)	$s_{u,II}$ (MPa)	G_{Ic} (N/mm)	**G_{IIc} (N/mm)**
210	**80.77**	**23**	**23**	**0.6**	**1.2**

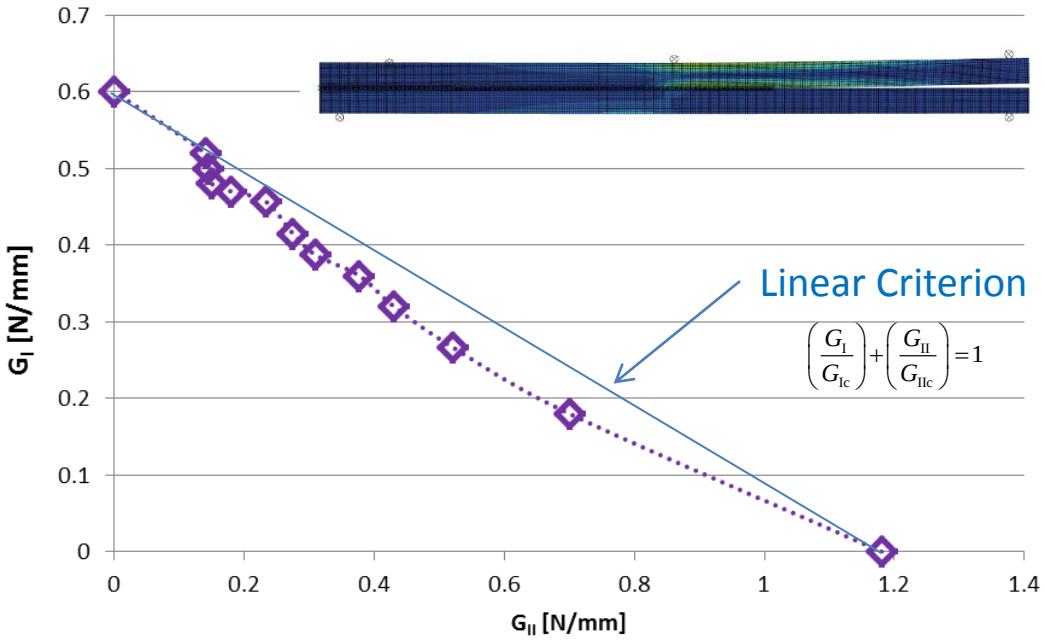

Numerical Fracture Envelope for MMB.

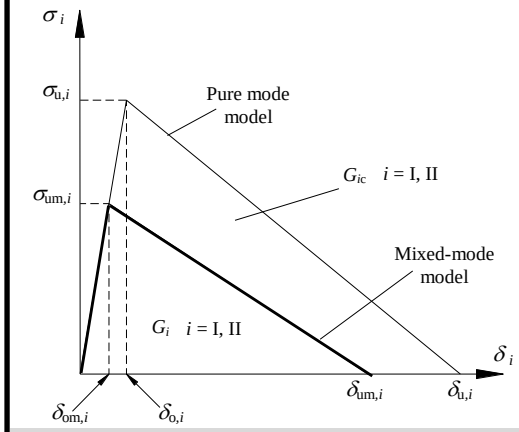

The linear softening law for pure and mixed-mode cohesive damage model.

$$\left(\frac{G_I}{G_{Ic}}\right)+\left(\frac{G_{II}}{G_{IIc}}\right)=1 \quad (3)$$

quadratic stress criterion to simulate damage initiation

$$\left(\frac{\sigma_I}{\sigma_{u,I}}\right)^2+\left(\frac{\sigma_{II}}{\sigma_{u,II}}\right)^2=1 \quad (4)$$

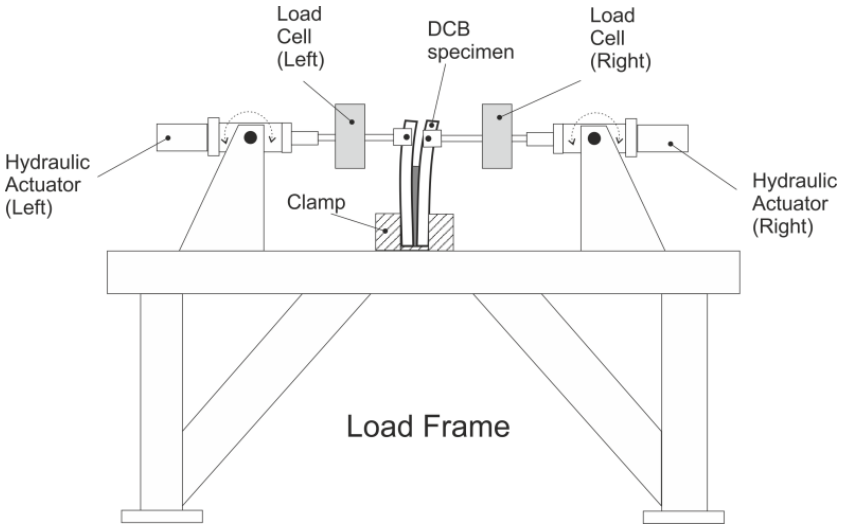

Numerical analysis of the dual actuator load test applied to fracture characterization of bonded joints

F.J.P. Chaves et al. / International Journal of Solids and Structures 48 (2011) 1572–15

$$G_I = \frac{6P_I^2}{B^2 h}\left(\frac{2a_{eI}^2}{h^2 E} + \frac{1}{5G}\right) \quad (5)$$

$$G_{II} = \frac{9P_{II}^2 a_{eII}^2}{4B^2 h^3 E} \quad (6)$$

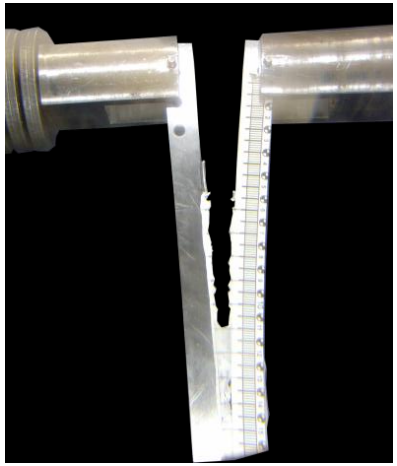

DAL loading a DCB specimen.

Different combinations of applied displacement rates provide different levels of mode ratios, thus allowing an easy definition of the fracture envelope in the G_I versus G_{II} space.

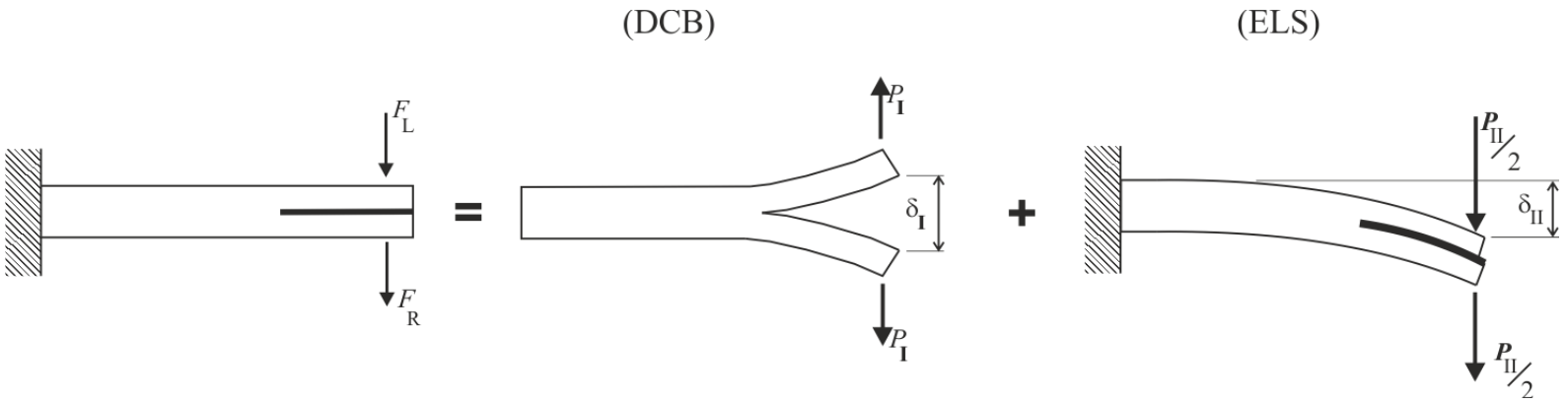

Schematic representation of loading for the DAL test.

pure mode loading

$$P_I = \frac{F_R - F_L}{2} \qquad P_{II} = F_R + F_L \qquad (7)$$

pure mode displacements

$$\delta_I = \delta_R - \delta_L \qquad \delta_{II} = \frac{\delta_R + \delta_L}{2} \qquad (8)$$

It is useful to define the displacement ratio

$$\lambda = \delta_L/\delta_R \qquad (9)$$

λ = -1 pure mode I

λ = 1 pure mode II

The specimen was modelled with 7680 plane strain 8-node quadrilateral elements and 480 6-node interface elements with null thickness placed at the mid-plane of the bonded specimen.

ABAQUS®

Elastic and cohesive properties.

Elastic properties (Steel)		Cohesive properties (Adhesive)			
E (GPa)	G (MPa)	$s_{u,I}$ (MPa)	$s_{u,II}$ (MPa)	G_{Ic} (N/mm)	**G_{IIc} (N/mm)**
210	**80.77**	**23**	**23**	**0.6**	**1.2**

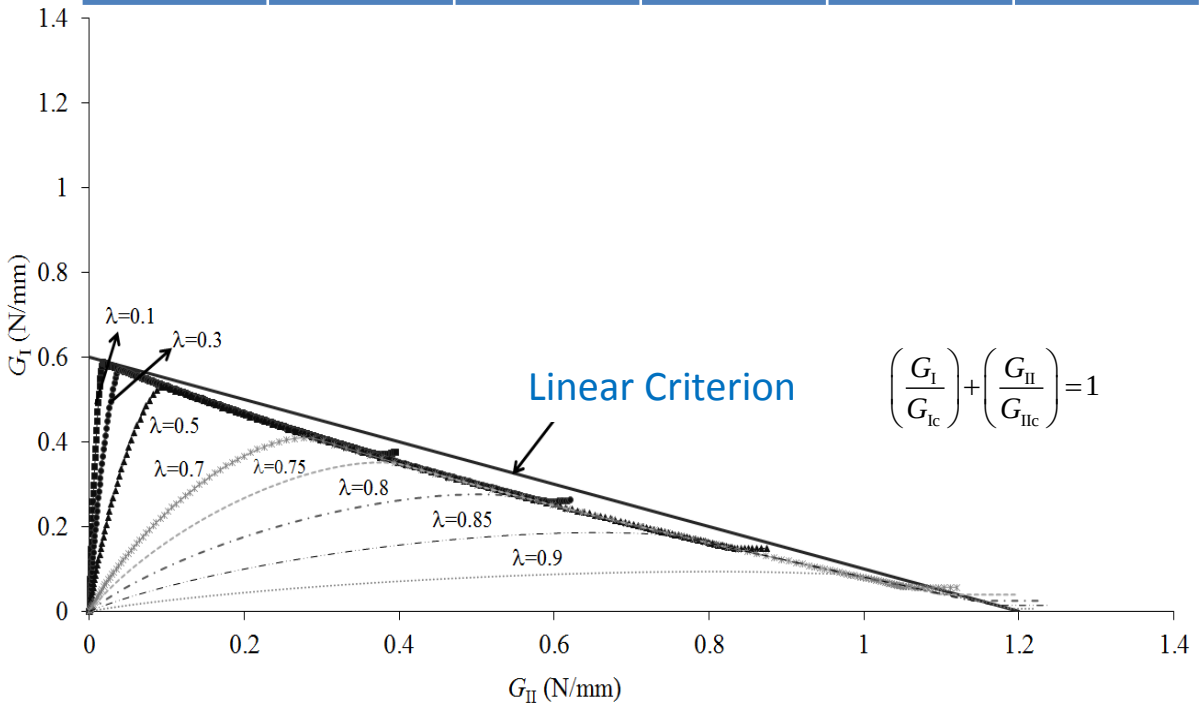

Numerical Fracture Envelope for DAL

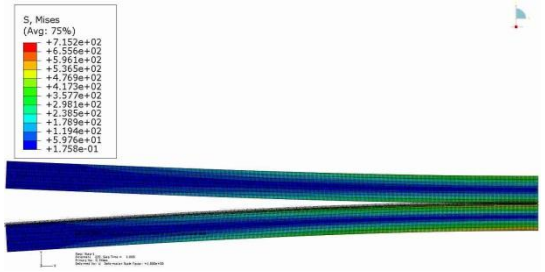

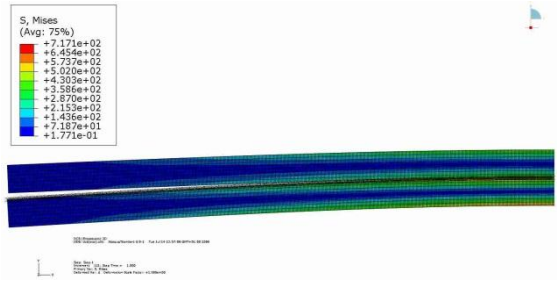

practically the entire fracture envelope can be obtained using only two combinations (λ = 0.1 and λ = 0.75) **important advantage of the DAL test**

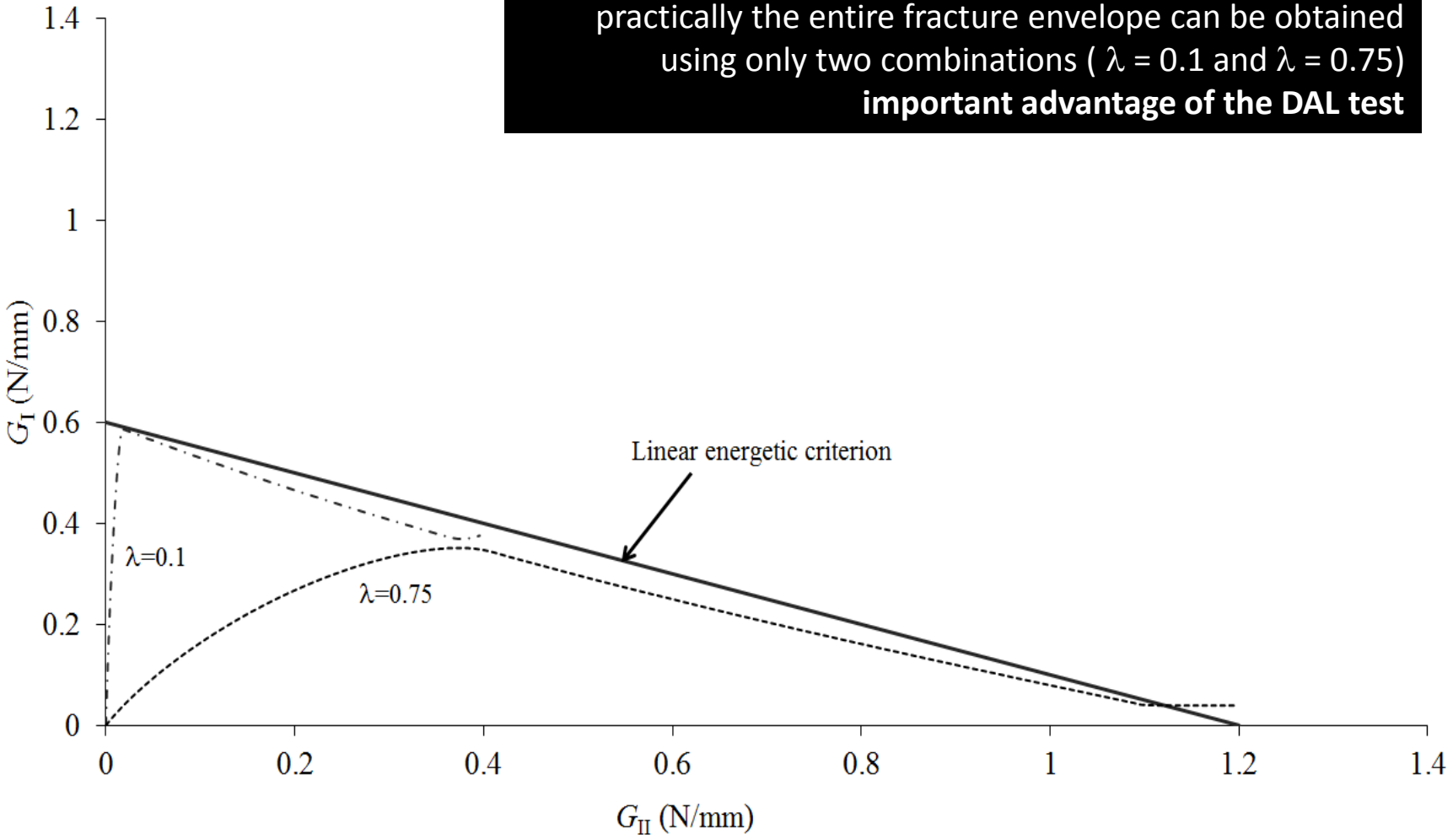

Plot of the G_I versus G_{II} strain energies for λ = 0.1 and λ = 0.75.

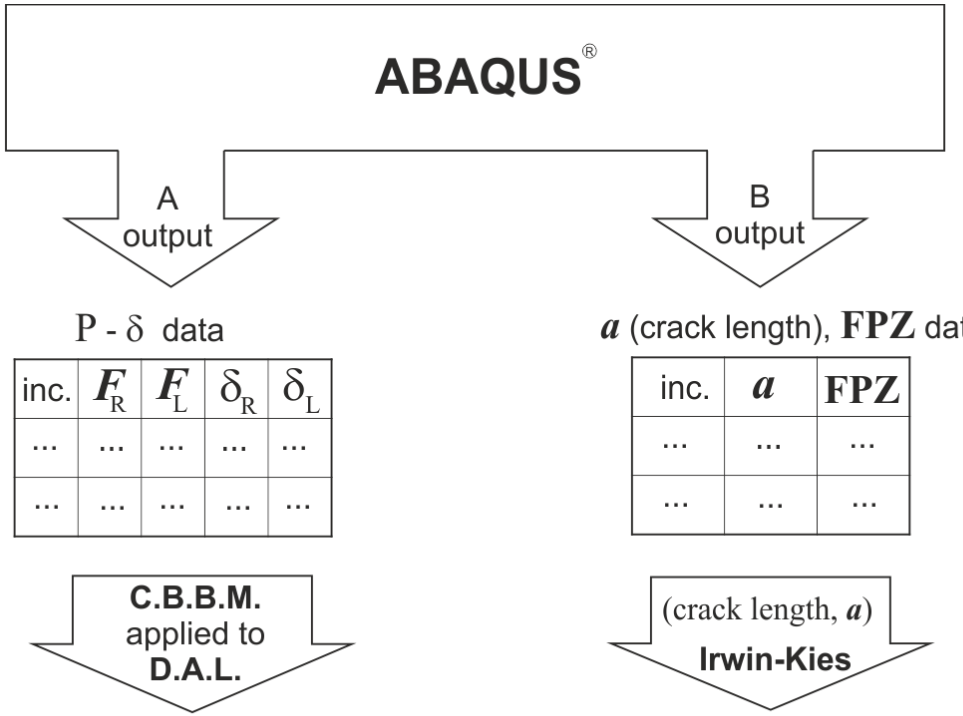

(5) & (6)

$$G_T = \frac{F_R^2}{2B}\frac{dC_R}{da} + \frac{F_L^2}{2B}\frac{dC_L}{da} \quad (10)$$

it can be concluded that both methods provide consistent results

agreement increases as the conditions of self-similar crack propagation become more evident.

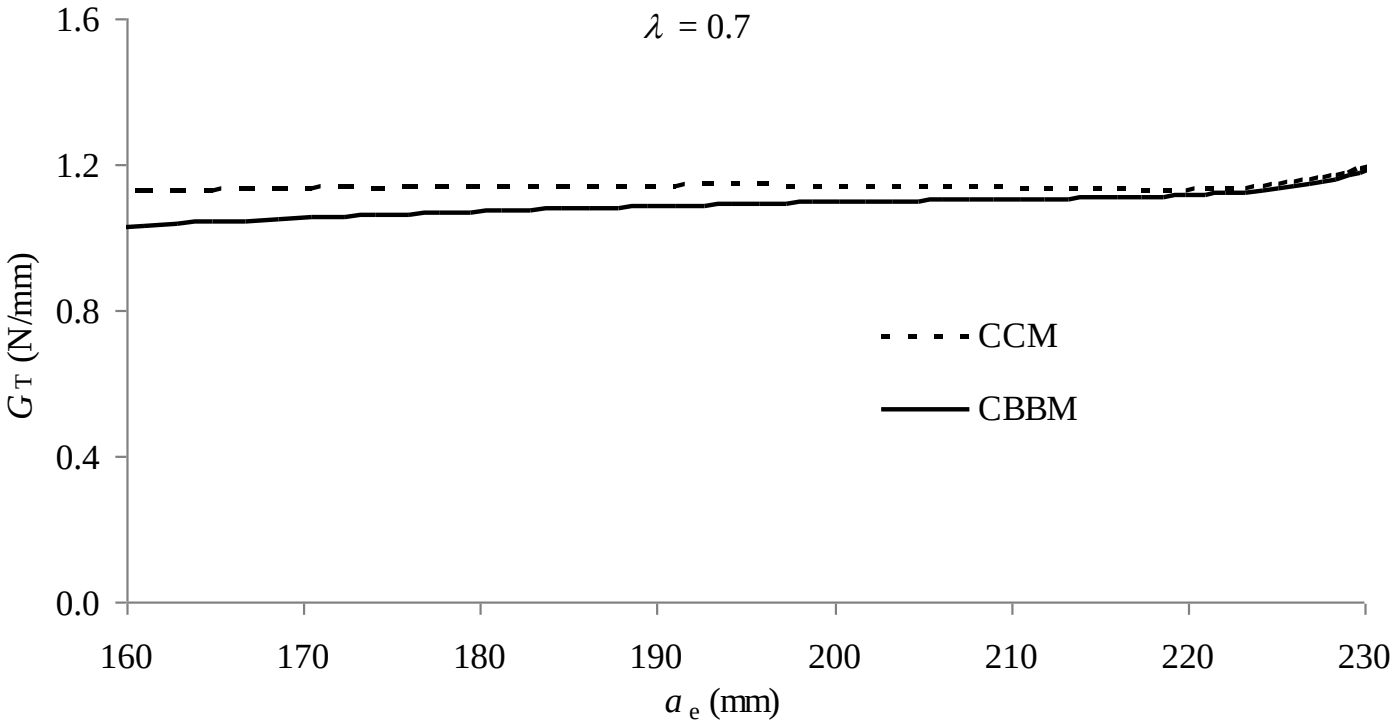

Plot of the G_T strain energy for $\lambda = 0.7$ obtained with CCM and CBBM.

N.B.: Although the CCM is a function of a, the a_e was used to provide better comparison between the two methods.

Mixed-mode testing is being implemented with a specimen load jig similar to the one that Spelt proposed, using DCB specimens used for the pure mode I (DCB) and pure mode II (ENF) and also for mixed-mode DAL

G. Fernlund & J. K. Spelt, *Composites Science and Technology* **50** (1994) 441-449

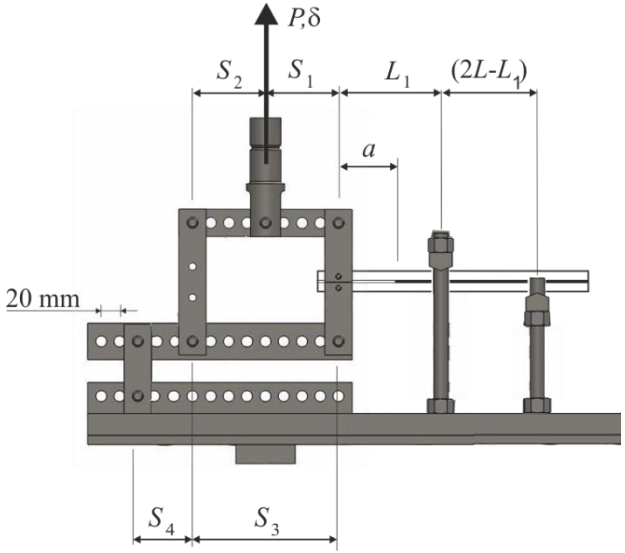

$$G_I = \frac{6\,P_I^2}{B^2 h}\left(\frac{2a_{e,I}^2}{h^2 E} + \frac{1}{5G}\right) \quad (11)$$

$$G_{II} = \frac{9\,P_{II}^2\,a_{e,II}^2}{4\,B^2 h^3 E} \quad (12)$$

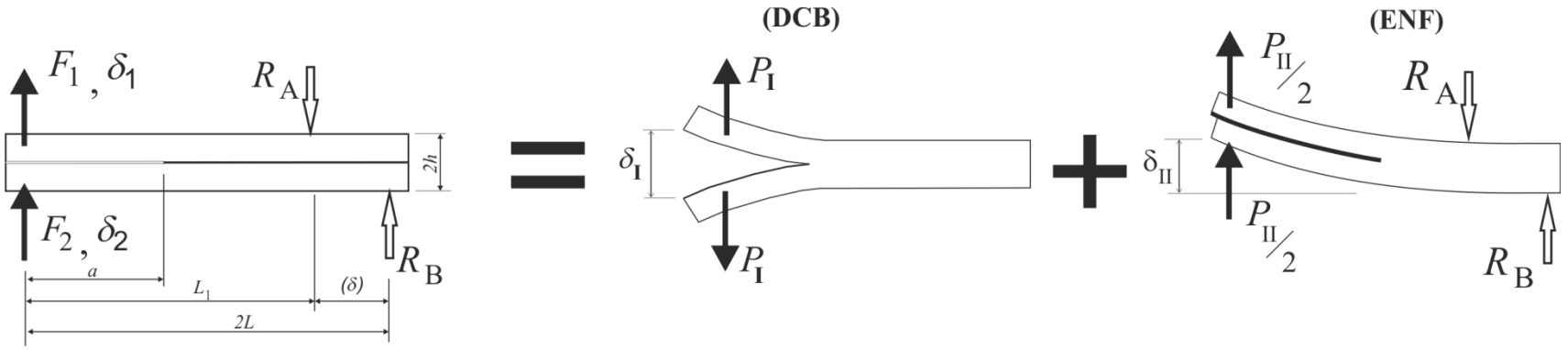

Schematic representation of loading for the SPELT test.

pure mode loading

$$P_I = \frac{F_1 - F_2}{2} \qquad P_{II} = F_1 + F_2 \tag{13}$$

pure mode displacements

$$\delta_I = \delta_1 - \delta_2 \qquad \delta_I = \frac{\delta_1 + \delta_2}{2} \tag{14}$$

$$R_A = \frac{2\,L\,P_{II}}{2L - L_1} \;\; and \;\; R_B = \frac{P_{II} L_I}{2L - L_1} \tag{15}$$

The specimen was modelled with 3992 plane strain 8-node quadrilateral elements and 382 6-node interface elements with null thickness placed at the mid-plane of the bonded specimen.

ABAQUS®

Elastic and cohesive properties.

Elastic properties (Steel)		Cohesive properties (Adhesive)			
E (GPa)	G (MPa)	$s_{u,I}$ (MPa)	$s_{u,II}$ (MPa)	G_{Ic} (N/mm)	**G_{IIc} (N/mm)**
210	**80.77**	**23**	**23**	**0.6**	**1.2**

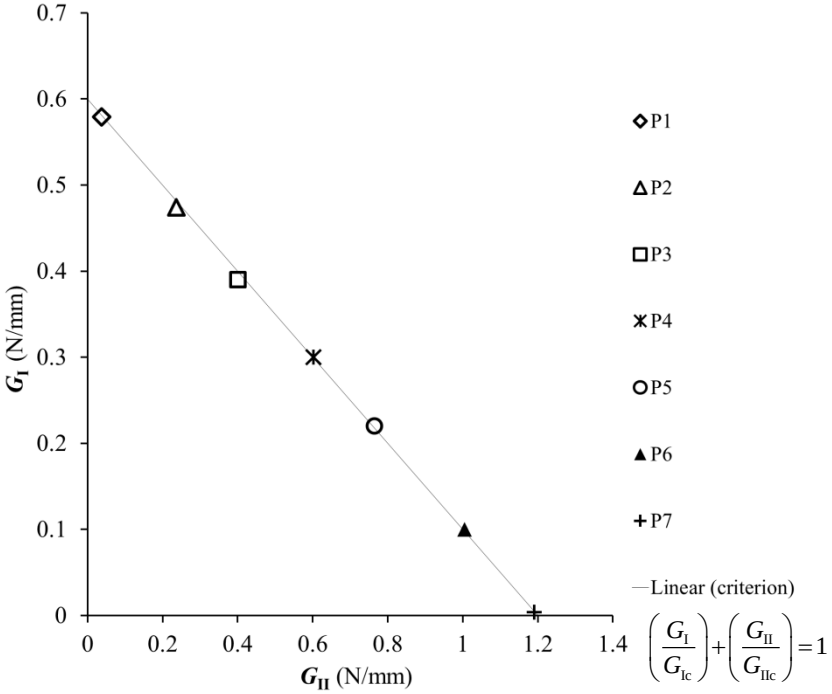

Numerical Fracture Envelope for SPELT

P1

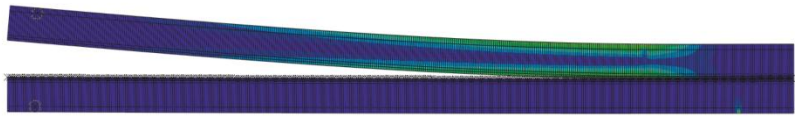

G_I/G_{II}=3.6

P3

G_I/G_{II}=1

P5

G_I/G_{II}=0.24

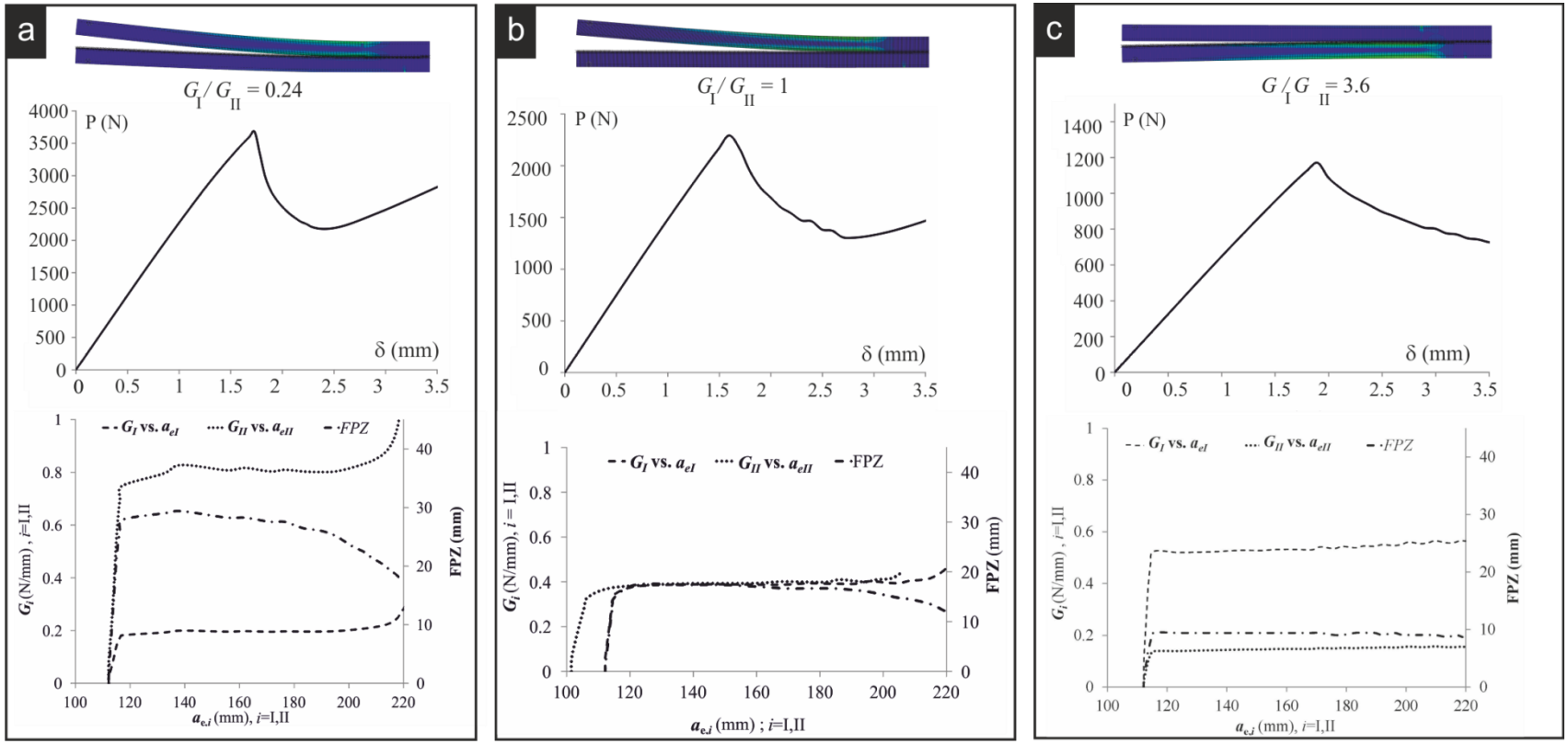

Deformed shapes, load-displacement curves and *R*-curves for three mixed-mode loadings.

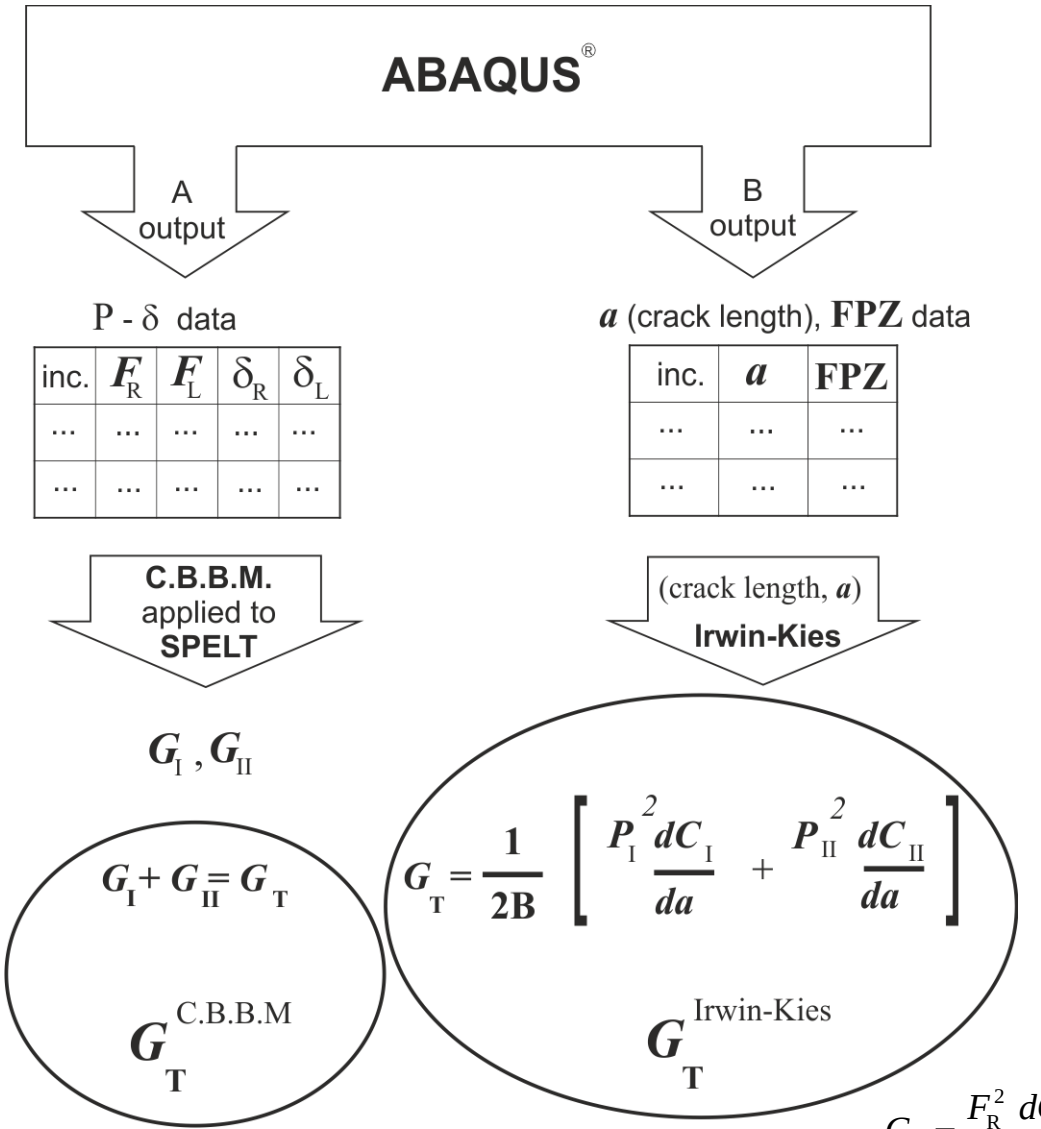

(11) & (12)

$$G_T = \frac{F_R^2}{2B}\frac{dC_R}{da} + \frac{F_L^2}{2B}\frac{dC_L}{da} \quad (10)$$

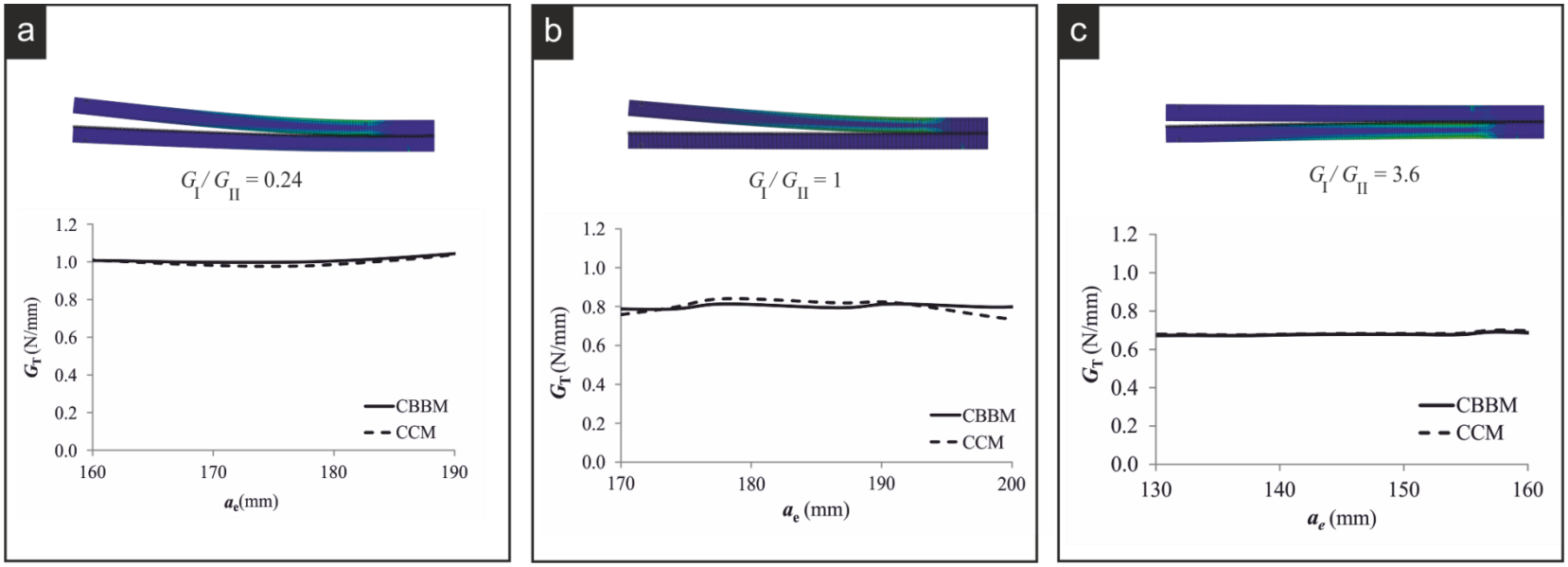

Plot of the $G_T = f(a_e)$ curves obtained by the CCM and the CBBM for G_I/G_{II}=0.24;1 and 3.6.

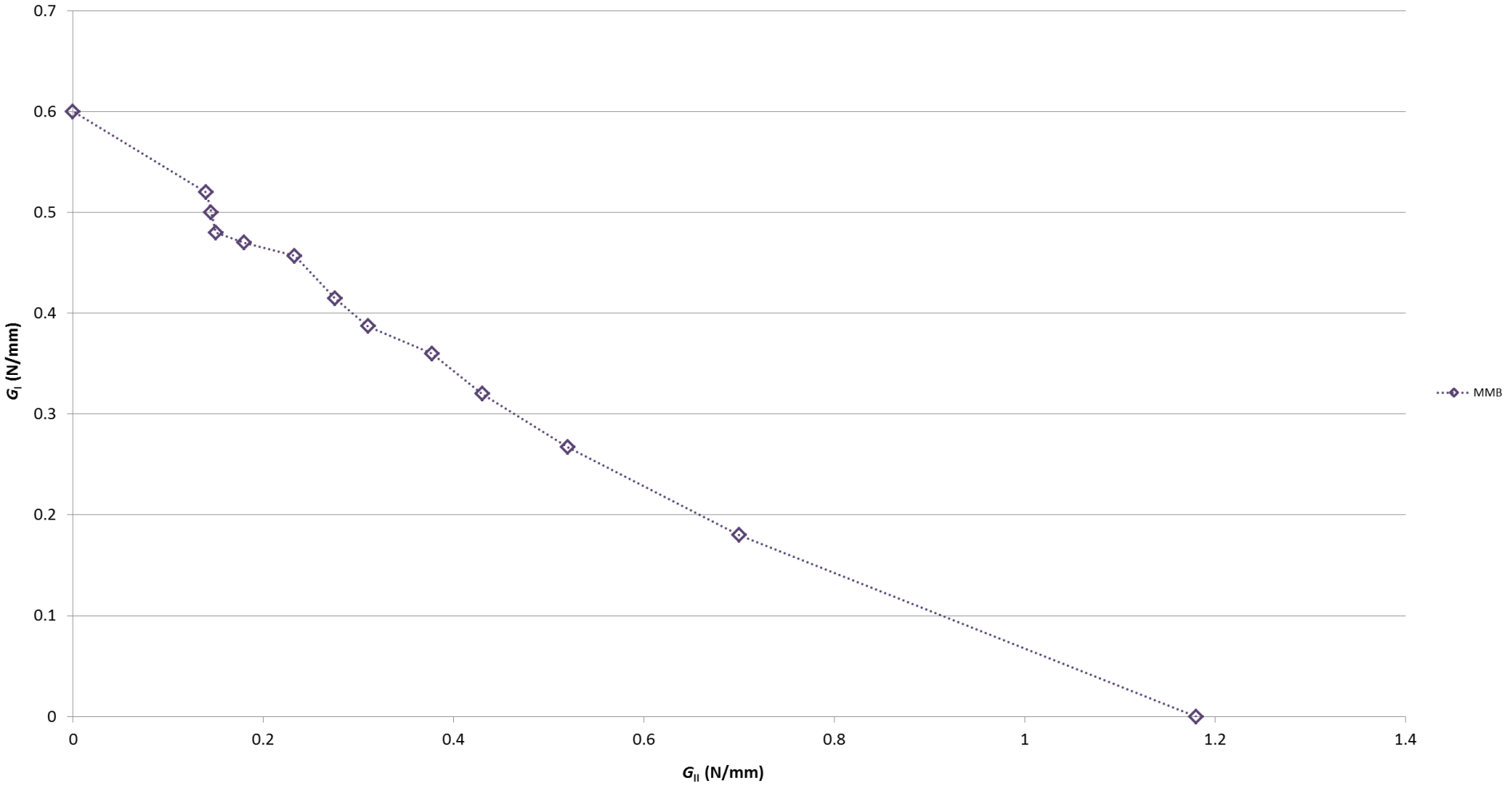

numerical envelope plot for MMB

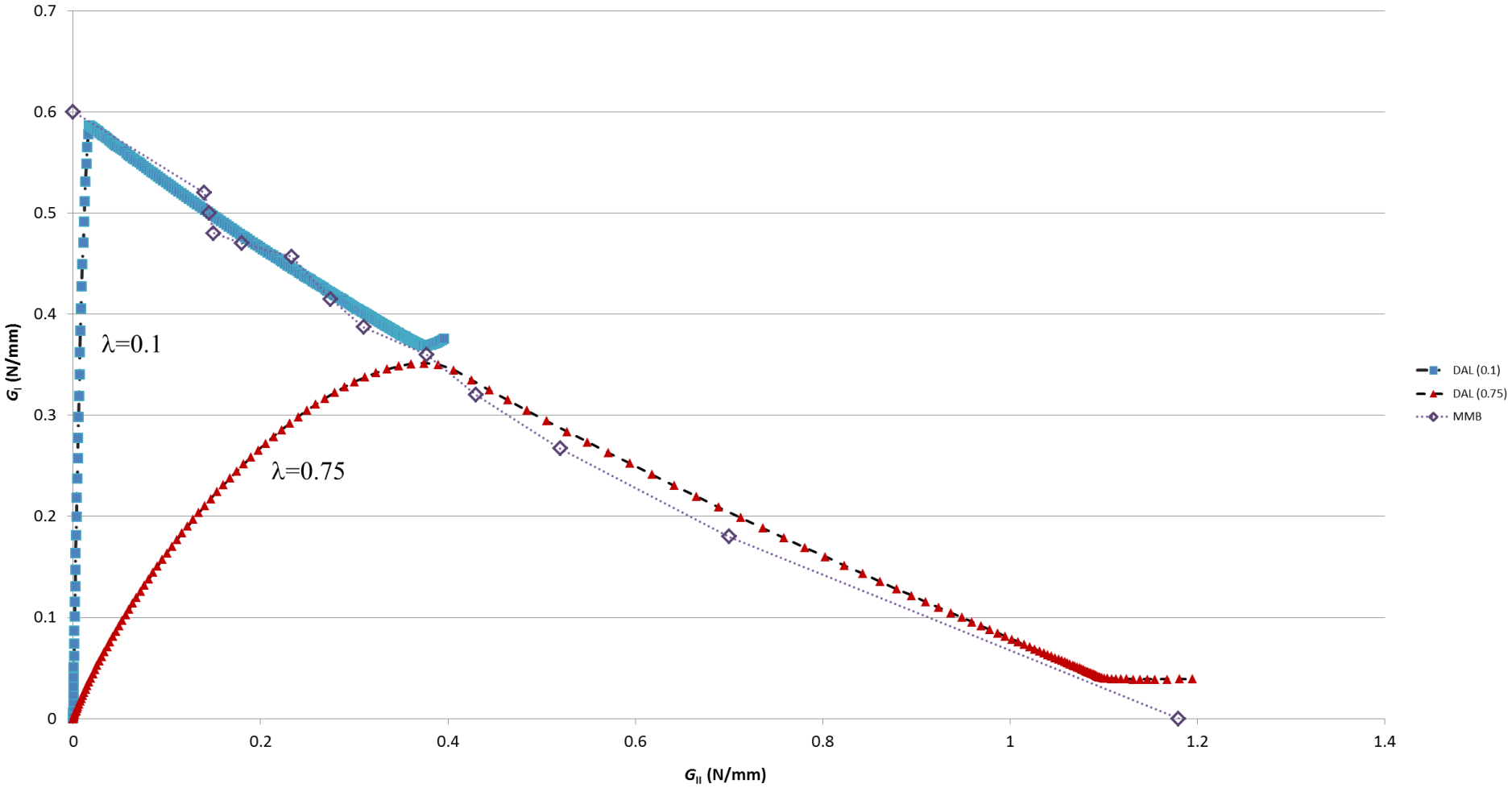

numerical envelope plot for MMB and DAL

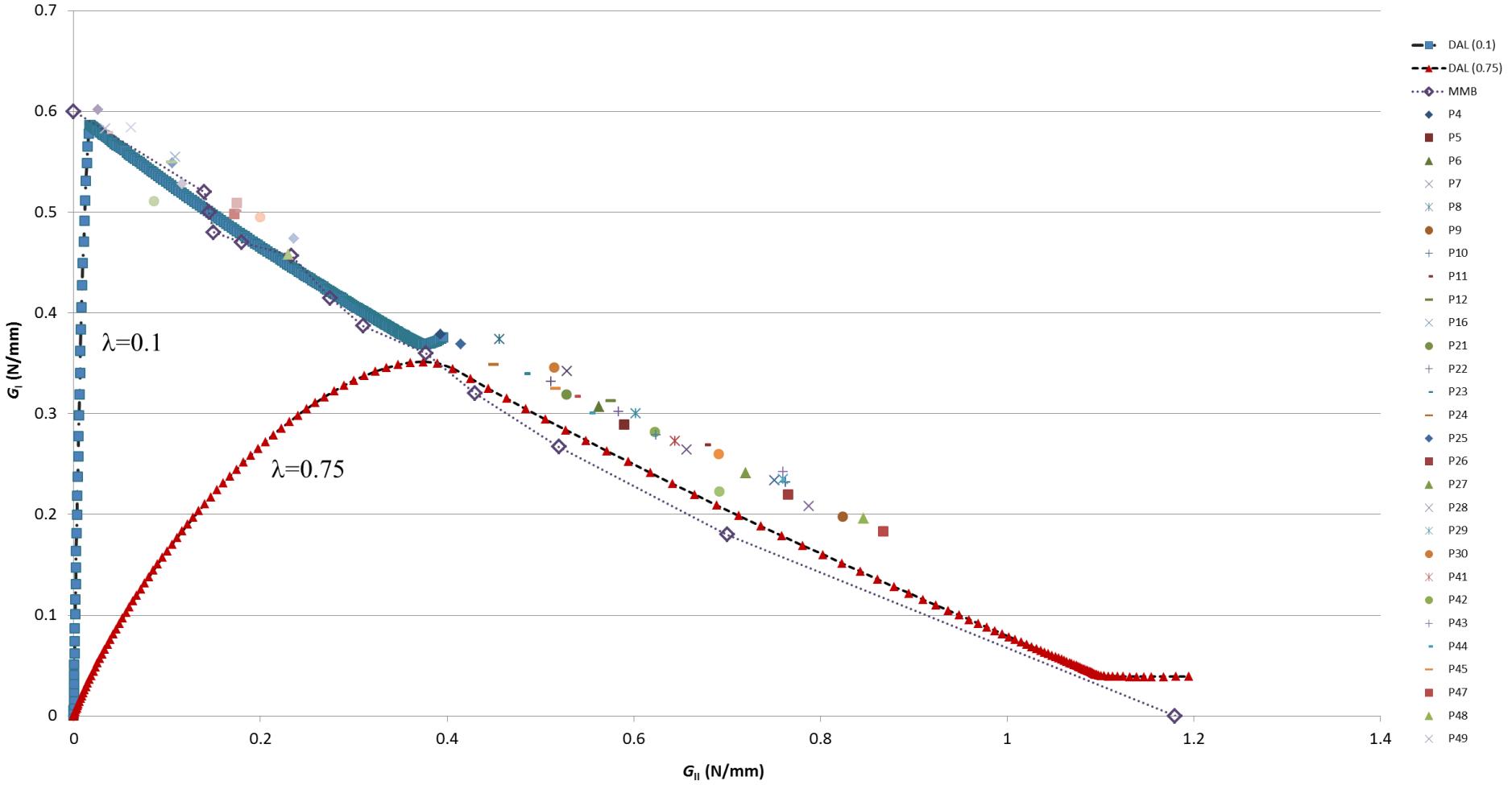

numerical envelope plot for MMB and DAL and SPELT

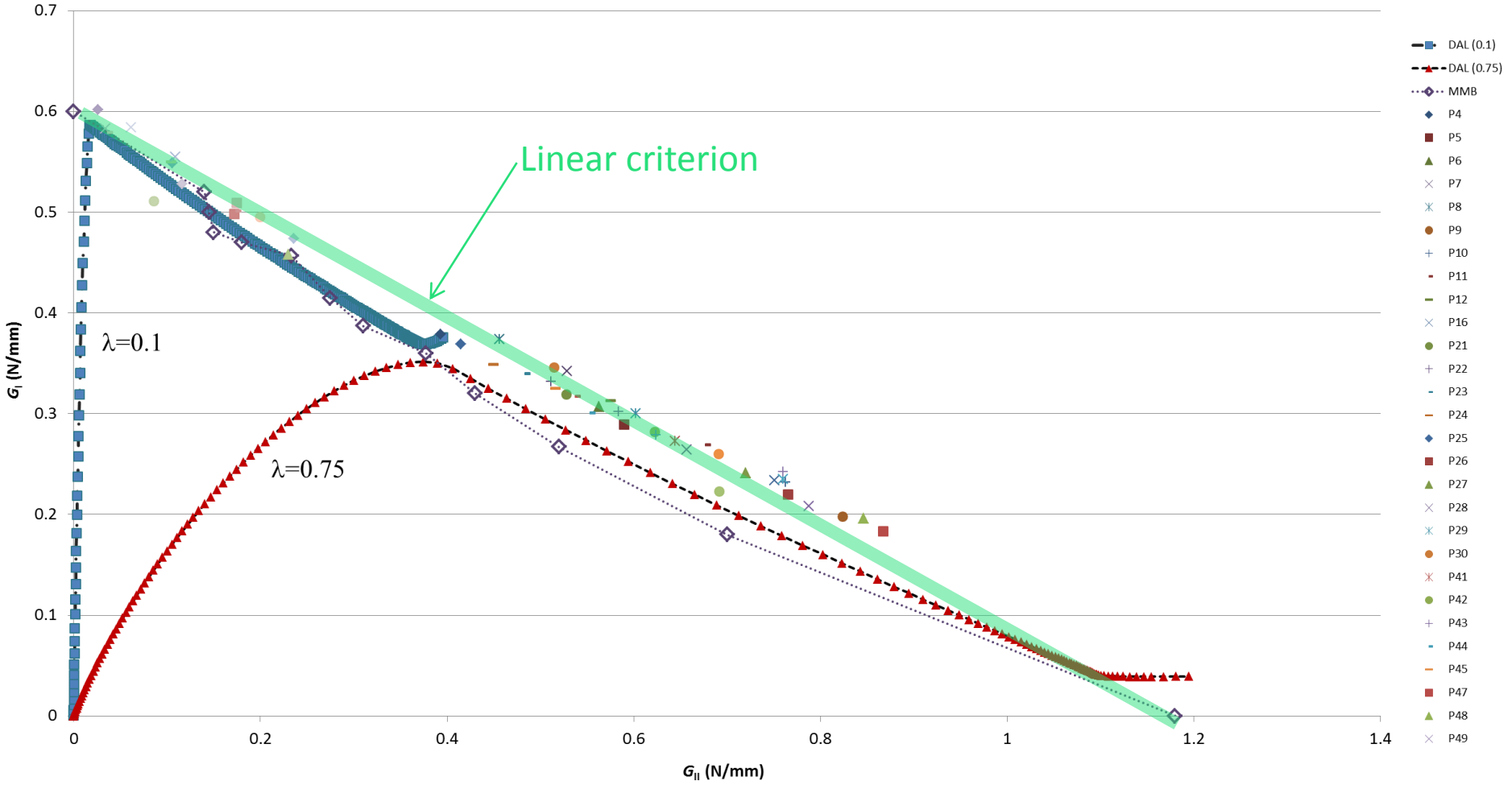

numerical envelope plot for MMB and DAL and SPELT

scenario P11

S1	S2	S3	S4
80	80	160	60

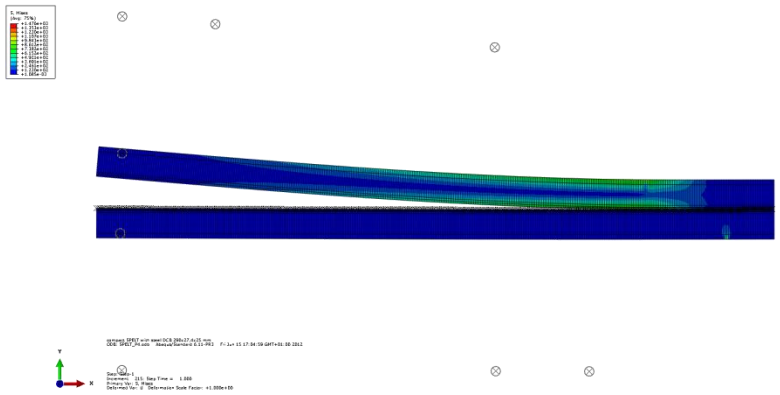

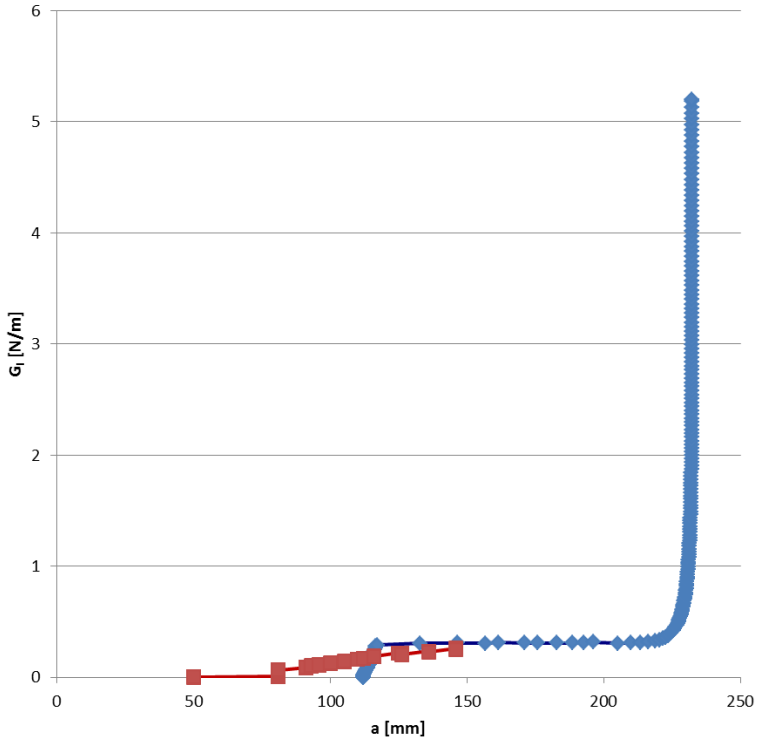

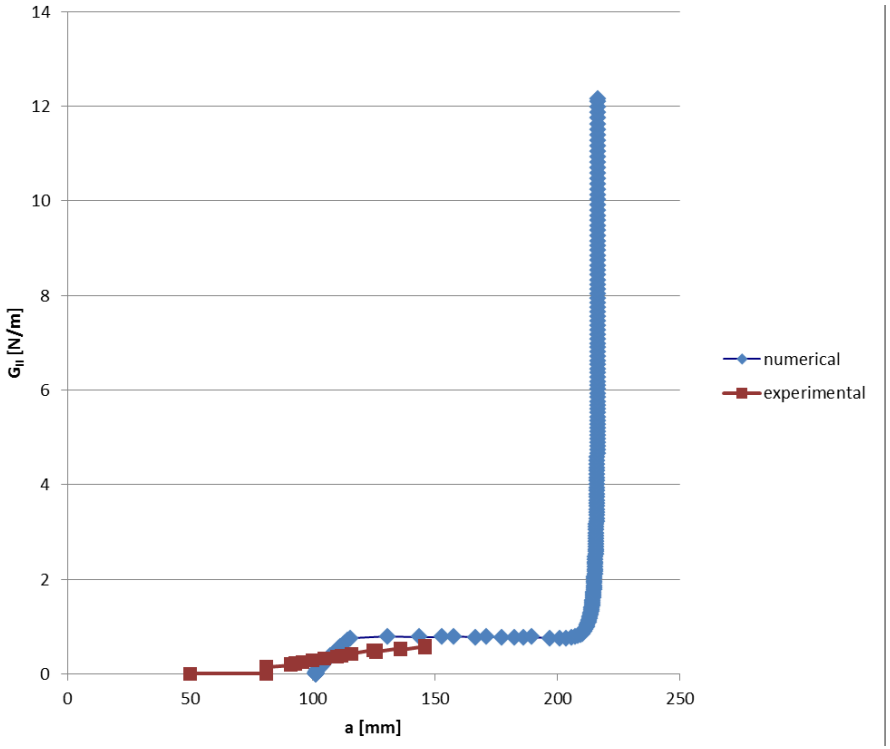

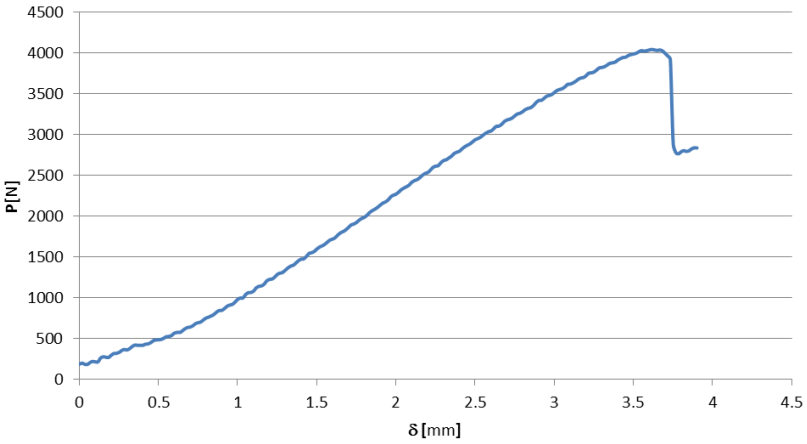

P-δ curve for $\Psi = 56^o$

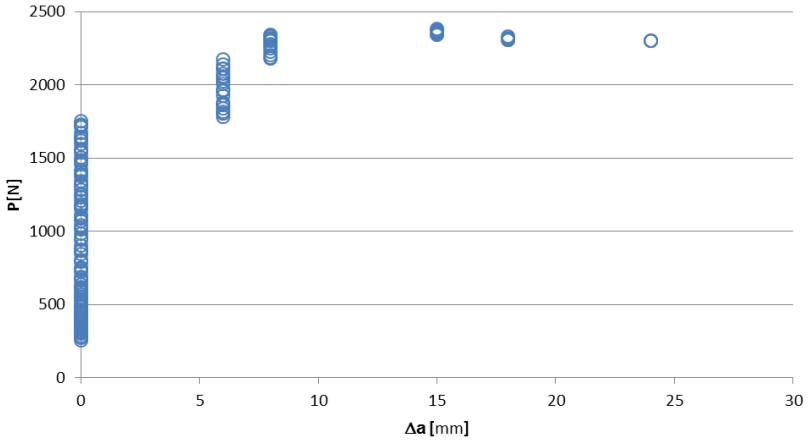

P-Δa curve for $\Psi = 56^o$

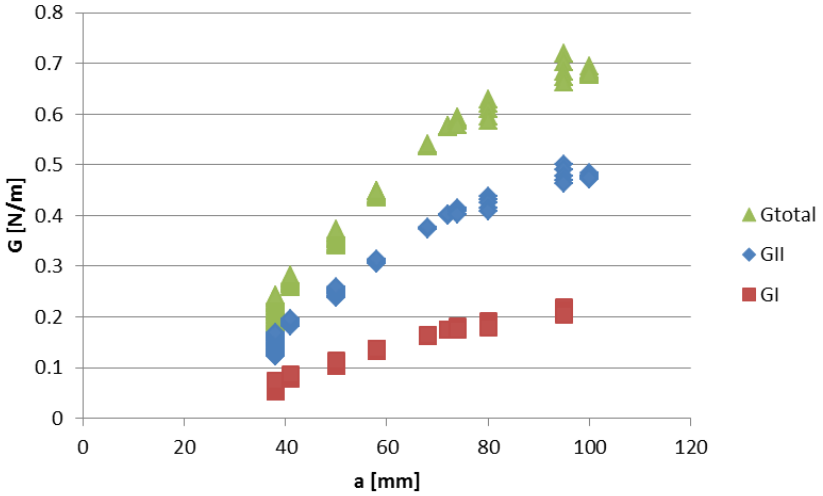

R curve for $\Psi = 56^o$

Araldite® 2015

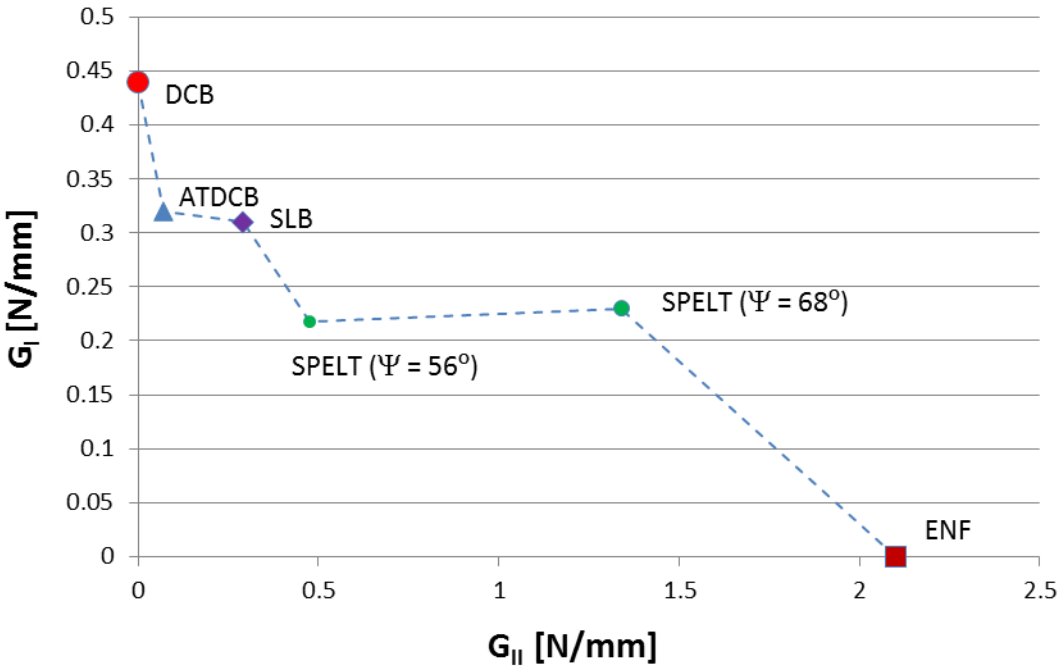

Experimental envelope (Araldite® 2015)

- a new data reduction scheme based on specimen compliance, beam theory and crack equivalent concept was proposed to overcome some problems intrinsic to the DAL and SPELT tests

- the model provides a simple mode partitioning method and does not require crack length monitoring during the test, which can lead to incorrect estimation of fracture energy due to measurement errors

- since the current compliance is used to estimate the equivalent crack length, the method is able to account indirectly for the presence of a non-negligible fracture process zone (very important for ductile adhesives)

- for pure modes I and II, excellent agreement was achieved with the fracture values inputted in the cohesive model

- for DAL tests a slight difference relative to the inputted linear energetic criterion was observed in the central region of the G_I versus G_{II} plot, corresponding to mixed-mode loading, which is attributed to the non self-similar crack propagation conditions that are more pronounced in these cases. The SPELT test has a nearly constant mixed-mode, providing better results for this central region of the fracture envelope.

- with the DAL test only two combinations of the displacement ratio are sufficient to cover almost all the fracture envelope

The authors would like to acknowledge the support of the National Science Foundation (DMR NSF 0415840) in the development of a dual actuator load frame capable of facilitating mixed mode fracture studies.

The authors also acknowledge the financial support of Fundação Luso Americana para o Desenvolvimento (FLAD) through project 314/06, 2007 , IDMEC and FEUP.

Thank you.

Using Timoshenko beam theory, the strain energy of the specimen due to bending and including shear effects is:

$$U = \int_0^a \frac{M_R^2}{2EI_R}dx + \int_0^a \frac{M_L^2}{2EI_L}dx + \int_a^L \frac{M_T^2}{2EI}dx + \int_0^a \int_{-h/2}^{h/2} \frac{\tau_R^2}{2G} B\,dydx + \int_0^a \int_{-h/2}^{h/2} \frac{\tau_L^2}{2G} B\,dydx + \int_a^L \int_{-h}^{h} \frac{\tau_T^2}{2G} B\,dydx \quad (16)$$

M is the bending moment

subscripts R and L stand for right and left adherends

T refers to the total bonded beam (of thickness 2*h*)

E is the longitudinal modulus

G is the shear modulus

B is the specimen and bond width

I is the second moment of area of the indicated section

For adherends with same thickness, considered in this analysis, $I = 8I_R = 8I_L$

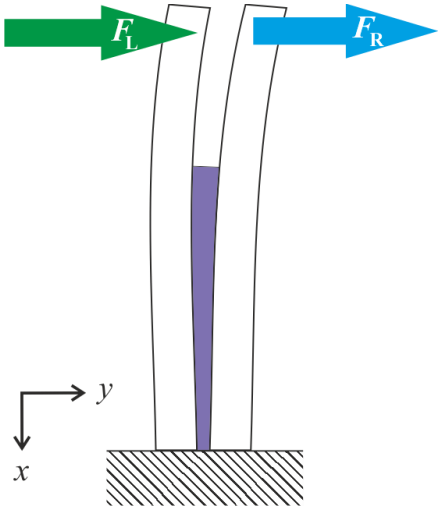

Schematic representation of loading in the DAL test.

The shear stresses induced by bending are given by:

$$\tau = \frac{3}{2}\frac{V}{Bh}\left(1-\frac{y^2}{c^2}\right) \qquad (17)$$

c - beam half-thickness

V - transverse load ⟶ on each arm for $0 \le x \le a$, and on total bonded beam for $a \le x \le L$

From Castigliano's theorem $\delta = \partial U / \partial P$

- P is the applied load
- δ is the resulting displacement at the same point

the displacements of the specimen arms can be written as

$$\delta_L = \frac{\left(7a^3+L^3\right)F_L}{2Bh^3E} + \frac{(L^3-a^3)F_R}{2Bh^3E} + \frac{3L\left[(F_L+F_R)+a(F_L-F_R)\right]}{5BhG}$$

$$\delta_R = \frac{\left(7a^3+L^3\right)F_R}{2Bh^3E} + \frac{(L^3-a^3)F_L}{2Bh^3E} + \frac{3L\left[(F_L+F_R)+a(F_R-F_L)\right]}{5BhG} \qquad (18)$$

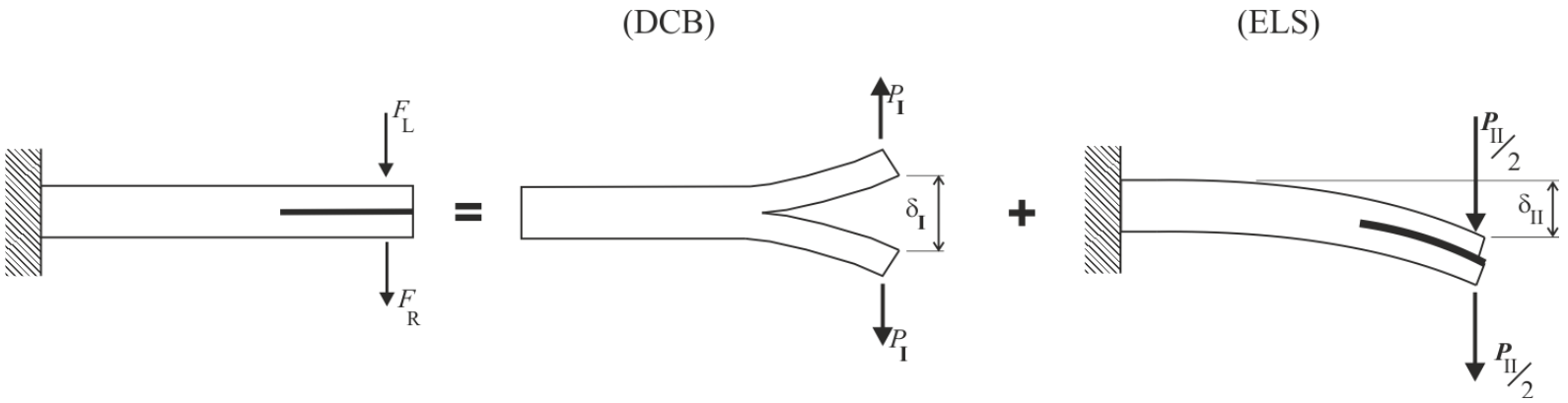

Figure 13. Schematic representation of loading in the DAL test.

pure mode loading

$$P_I = \frac{F_R - F_L}{2} \qquad P_{II} = F_R + F_L \tag{13}$$

pure mode displacements

$$\delta_I = \delta_R - \delta_L \qquad \delta_{II} = \frac{\delta_R + \delta_L}{2} \tag{14}$$

Combining equations (3-5), the pure mode compliances become

(19) $$C_{\mathrm{I}} = \frac{\delta_{\mathrm{I}}}{P_I} = \frac{8a^3}{Bh^3E} + \frac{12a}{5BhG}$$ and $$C_{\mathrm{II}} = \frac{\delta_{\mathrm{II}}}{P_{\mathrm{II}}} = \frac{3a^3 + L^3}{2Bh^3E} + \frac{3L}{5BhG}$$ (20)

However, stress concentrations, root rotation effects, the presence of the adhesive, load frame flexibility, and the existence of a non-negligible fracture process zone ahead of crack tip during propagation are not included in these equations

To overcome these drawbacks, equivalent crack lengths can be calculated from the current compliances C_{I} and C_{II} (eq. 19 and 20)

$$\alpha a_{\mathrm{eI}}^3 + \beta a_{\mathrm{eI}} + \gamma = 0$$

$$a_{\mathrm{eI}} = \frac{1}{6\alpha} A - \frac{2\beta}{A} \quad (21)$$

$$a_{\mathrm{eII}} = \left[\left(C_{\mathrm{II}} - \frac{3L}{5BhG} \right) \frac{2Bh^3E}{3} - \frac{L^3}{3} \right]^{1/3} \quad (22)$$

$$\alpha = \frac{8}{Bh^3E}; \quad \beta = \frac{12}{5BhG}; \quad \gamma = -C_{\mathrm{I}}$$

$$A = \left(\left(-108\gamma + 12\sqrt{3\left(\frac{4\beta^3 + 27\gamma^2\alpha}{\alpha} \right)} \right) \alpha^2 \right)^{\frac{1}{3}}$$

The strain energy release rate components can be determined using the Irwin-Kies equation:

(23) $$G = \frac{P^2}{2B}\frac{dC}{da}$$

combined with equation 19 →

$$C_{\mathrm{I}} = \frac{\delta_{\mathrm{I}}}{P_I} = \frac{8a^3}{Bh^3E} + \frac{12a}{5BhG}$$

$$G_{\mathrm{I}} = \frac{6P_{\mathrm{I}}^2}{B^2h}\left(\frac{2a_{\mathrm{eI}}^2}{h^2E} + \frac{1}{5G}\right) \quad (11)$$

combined with equation 20 →

$$C_{\mathrm{II}} = \frac{\delta_{\mathrm{II}}}{P_{\mathrm{II}}} = \frac{3a^3 + L^3}{2Bh^3E} + \frac{3L}{5BhG}$$

$$G_{\mathrm{II}} = \frac{9P_{\mathrm{II}}^2 a_{\mathrm{eII}}^2}{4B^2h^3E} \quad (12)$$

- The method only requires the data given in the load-displacement (P-δ) curves of the two specimen arms registered during the experimental test.
- Accounts for the Fracture Process Zone (FPZ) effects, since it is based on current specimen compliance which is influenced by the presence of the FPZ.

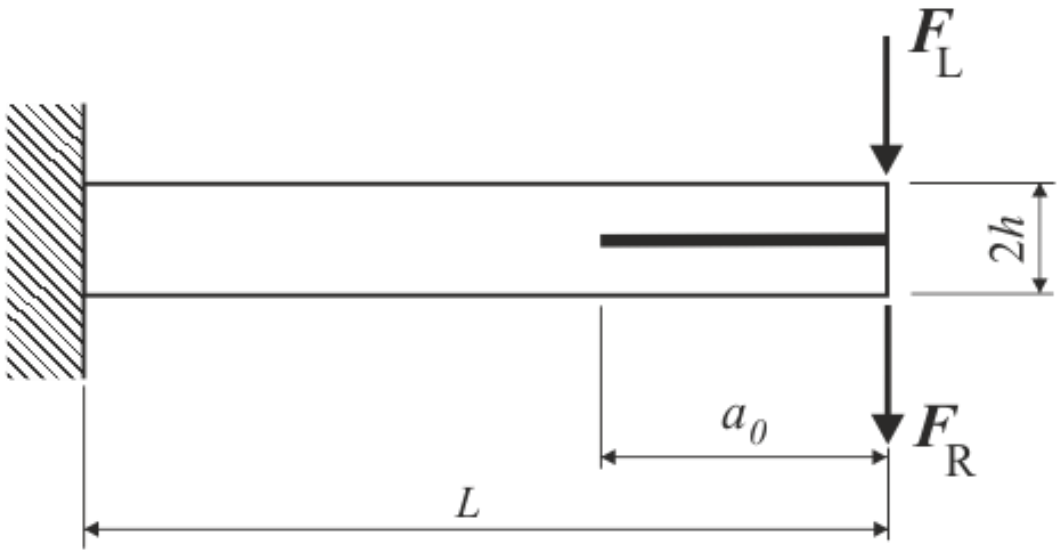

a_0=70 [mm]

B =25 [mm]

h =12.7 [mm]

L =250 [mm]